Conflict, poverty and water management issues exposing vulnerable communities in Africa to extreme floods that are now common events because of climate change

Authors

Izidine Pinto, *Royal Netherlands Meteorological Institute (KNMI), De Bilt, The Netherlands*
Ben Clarke, *Centre for Environmental Policy, Imperial College London, UK*
Sjoukje Philip, *Royal Netherlands Meteorological Institute (KNMI), De Bilt, The Netherlands*
Sarah Kew, *Royal Netherlands Meteorological Institute (KNMI), De Bilt, The Netherlands*
Maja Vahlberg, *Red Cross Red Crescent Climate Centre, The Hague, the Netherlands; Swedish Red Cross, Stockholm, Sweden (based in Ubmeje/Umeå, Sweden)*
Zinzi Horne, *Red Cross Red Crescent Climate Centre, The Hague, The Netherlands (based in Kingstown, Saint Vincent and the Grenadines)*
Roop Singh, *Red Cross Red Crescent Climate Centre, The Hague, The Netherlands (based in New Jersey, USA)*
Abuelgasim I. I. Musa, *Sudan Meteorological Authority (SMA), Khartoum, Sudan*
Rabah Farah, *Sudan Meteorological Authority (SMA), Khartoum, Sudan*
Amira N. Mostafa, *Egyptian Meteorological Authority, Cairo, Egypt*
Friederike Otto, *Centre for Environmental Policy, Imperial College, London, UK*

Review authors

Clair Barnes, *Centre for Environmental Policy, Imperial College, London, UK*
Joyce Kimutai, *Centre for Environmental Policy, Imperial College, London, UK*

Main findings

- The severe floods of 2024 hit an extremely vulnerable region, and have significantly deepened a complex humanitarian crisis in Sudan, straining the capabilities of aid organisations and government bodies to respond.

- Similar to the findings for the Lake Chad and Niger Basin, the event in Sudan is not rare in today's climate, which is 1.3°C warmer than it would have been at the beginning of the industrial period. An event of this magnitude is expected to occur about once every 3 years in Sudan, whereas the Lake Chad event had a return time of 10 years and the Niger event is expected on average once every 5 years.
- To assess if human-induced climate change influenced the heavy rainfall in Sudan, we first determine if there is a trend in the observations. Results showed that observed 30-day rainfall intensity has increased in intensity by about 18% since 1981 over the study region.
- To quantify the role of human-induced climate change we also analyse climate models over the relatively small study region. Overall, the available climate models indicate about a doubling in the likelihood of an event such as the one under study with about 10% increase in intensity. Although the uncertainty is large, the majority of the models indicate a trend toward more extreme precipitation events. Again, these results are comparable to the ones obtained in the Lake Chad and Niger Basin study, where we found similar changes for the Niger Basin, and an even larger increase due to human-induced warming for the Lake Chad Basin.
- Under a future warming scenario where the global temperature is 2°C higher than pre-industrial levels, climate models suggest that even wetter 30-day periods should be expected. Given that these events are not rare today, this means they will be common occurrences, and the region needs to prepare for much heavier events than those observed in 2024. These studies highlight that there is an urgent need to drastically improve water management and reduce vulnerability to seasonal rainfall.
- Ongoing conflict and fragility is acting as a risk multiplier, on top of the existing issues of poverty, rapid urbanisation, and ageing infrastructure. In particular, conflict has created a displacement crisis in the region with millions displaced in Chad, Nigeria and Sudan, living in makeshift shelters and at higher risk when extreme rainfall triggers flooding.
- The transboundary nature of the river systems in sub-saharan Africa requires coordination between neighbouring countries, which has been strained and hinders comprehensive flood management and early warning systems. Only a fraction of the population are known to have been aware of early warnings in the 2022 floods, likely to be the case in the 2024 floods. In addition, many of the same regions that were impacted by the 2022 floods had not fully recovered before they were hit again by the 2024 floods.
- The low return-period of the rainfall that resulted in such severe impacts underscores the chronic, deep vulnerabilities that are driving impacts. Together, these issues create a recipe for disaster, especially as even stronger rainfall events are to be expected in the future.
- To reduce flood risks, rehabilitation of damaged infrastructure should prioritise climate-smart design, including incorporating resilient materials and construction techniques and limiting construction in flood-prone areas. Effective water management, including maintaining and updating vital infrastructure like Arba'at, is crucial for mitigating both flood risks but also cascading risks on health. Finally, strengthening early warning systems by improving transboundary data sharing and ensuring greater access to warning and risk information, will be essential to reduce loss of life.

1 Introduction

From July up until the end of September 2024 most countries in and adjacent to the Sahel region experienced incredibly deadly floods.

In August, extreme rainfall led to catastrophic floods in Sudan. At least 205 people have lost their lives (AA, 2024) and more than 130,000 people have been displaced, with nearly half being people who were already displaced due the ongoing civil war (IOM, 2024). In September, further West in the Sahel region, floods killed more than 760 people in Nigeria, 330 in Niger and 30 in Cameroon (European Commission, 2024; ECHO, 2024).

The impacts of flooding largely undermine the food system and exacerbate the situation of acute food security in countries like Chad and Nigeria where there are multidimensional crises linked to conflict, and economic and climate shocks (FAO, 2024, 17 Oct). Approximately half of all those affected by flooding—about 1.5 million people—reside in Chad, a country already grappling with various security and humanitarian challenges (USAID, 2024, 18 Sep). These include armed group activities and the responsibility of hosting over one million refugees, nearly 640,000 of whom have fled conflict in neighbouring Sudan since April 2023 (USAID, 2024, 18 Sep). By October 1, 2024, nearly two million people in Chad had been affected by impacts like livelihood disruption, displacement and loss of infrastructure from the flood emergency (OCHA, 2024, 9 Oct). The situation is similar in Nigeria where there are currently 3.6 million internally displaced people, mainly in the northeast and the country has nearly 100,000 asylum-seekers and refugees within its borders (UN News, 2024, 17 Sep).

Public health risks have also been exacerbated by the flooding. A cholera outbreak, declared in August 2024, has spread more rapidly due to stagnant floodwaters, affecting over 2,900 people and resulting in 112 deaths across five states, including Kassala and River Nile (OCHA, 2024, 5 Sept). The destruction of roads and bridges has hampered the delivery of medical supplies, further straining response efforts. North Darfur, particularly the Zamzam IDP camp near Al Fasher, faces confirmed famine, marking the first global famine declaration since 2017 (OCHA, 2024, 1 Sept). The flood crisis has also deepened famine conditions in affected areas. Floodwaters have destroyed annual crop stocks, undermining livelihoods dependent on agriculture and daily wage labour (OCHA, 2024, 25 Aug).

The floods in Nigeria, Niger, Chad and Cameroon are nearly identical to the floods that hit the same region at the same time of the year in 2022, killing 612 people in Nigeria and 195 in Niger (Africa News, 2022; Ruth, 2022; Akbarzai et al. 2022).

In 2022 the World Weather Attribution initiative undertook an attribution study (WWA, 2022), looking at two regions: the lower Niger catchment and the lake Chad basin (see fig. 1 & 2). When comparing the rainfall in 2022 with that in 2024, we find that the spatial pattern as well as magnitude are very similar, with 2024 showing slightly higher amounts in the Lake Chad basin and slightly lower in the Niger basin. A repeat of the 2022 floods only two years later is not surprising and in line with our previous study which found that extreme rainfall events of this type are no longer rare events due to human-caused climate change. Our study found that similarly extreme 7-day rainfall events are expected to occur on average about once every 5 years in today's climate in the lower Niger Basin and that climate change has made such events approximately 5% more intense. In the Lake Chad Basin,

very wet seasons like this are expected to occur once every 10 years in today's climate and are made approximately 20% more intense by human-induced climate change. We do not need to carry out another attribution study to understand the contribution of climate change to the 2024 event in this region, as the results would be extremely similar to those of the 2022 study, given that the observational data sets and models have not changed other than adding two more years worth of data. However, it is clear that the catastrophic flooding experienced in Nigeria, Niger and Cameroon was exacerbated by climate change.

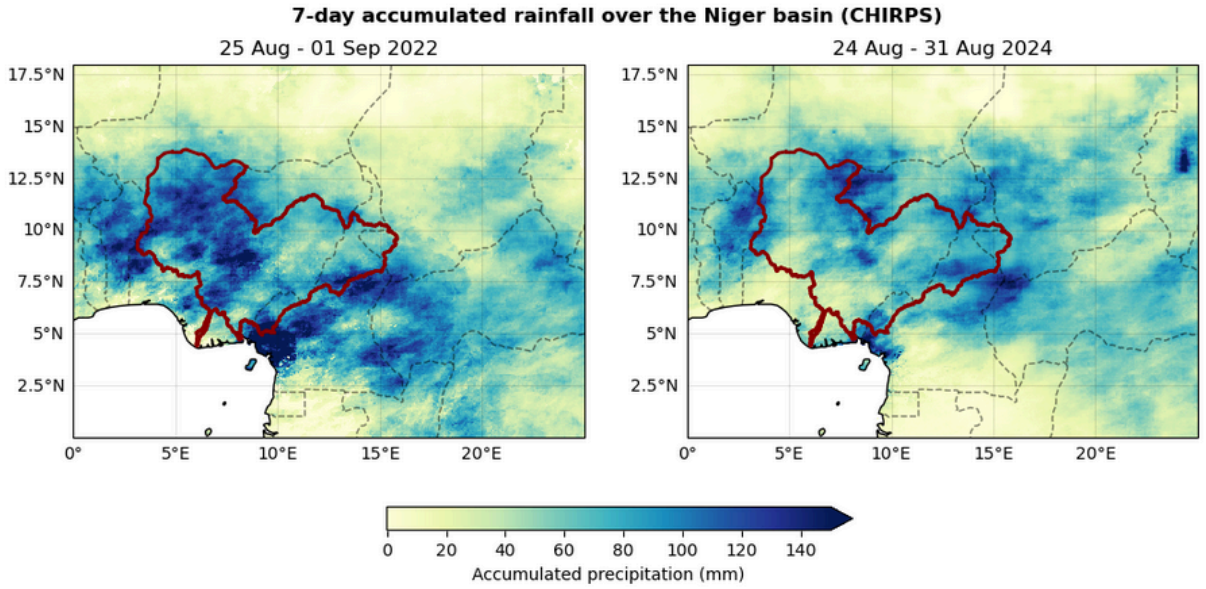

Fig 1. Observed mean daily precipitation from 26 Aug-1 Sep, 2022, and the 24 Aug - 31 Aug, 2024. The red highlight shows the Lower Niger catchment the wettest 7-day period over the Lower Niger catchment in JJAS in each year. Observations are taken from the CHIRPS dataset described in Section 2.1.

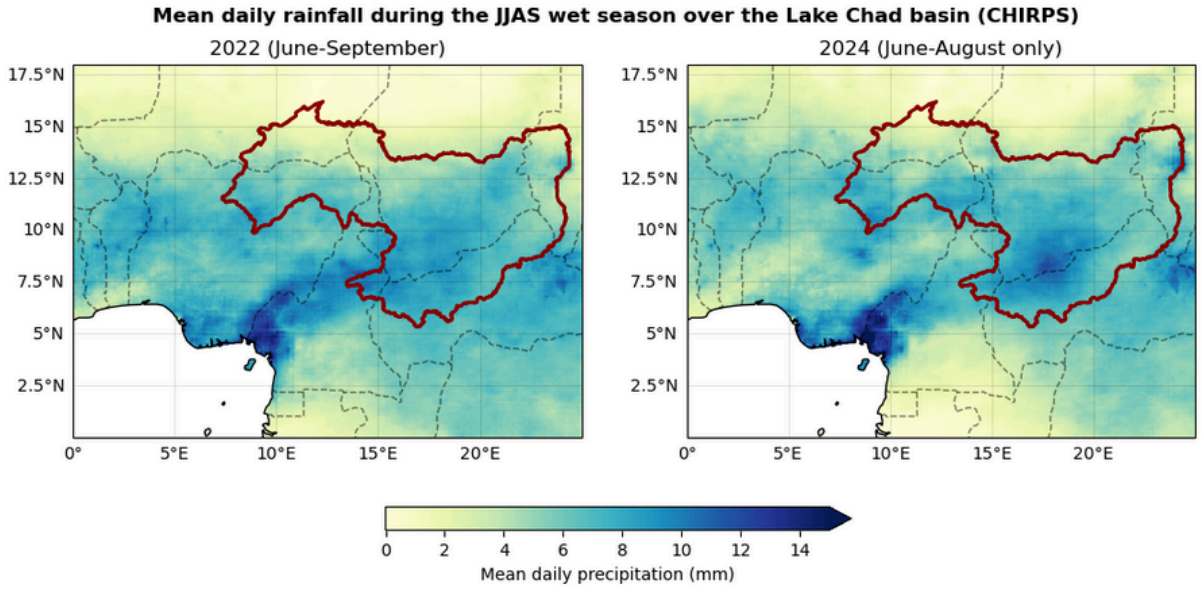

Fig 2. Observed average JJAS rainfall in the year a) 2022 and the year b) 2024. The red highlight shows the Lake Chad catchment Observations are taken from the CHIRPS dataset described in Section 2.1.

Instead we undertake an attribution study on the 2024 event in Sudan where, given the geographic location further to the east and with it a much stronger influence of the easterly jet and weaker dependence on West African monsoon, it is not a priori clear that the role of climate change in the heavy rainfall will be the same.

In the main findings we highlight findings that are relevant for the disastrous floods across all regions, as well as findings specific to Sudan. We particularly highlight similarities and differences in Vulnerability and Exposure in section 7 and the key findings.

1.1 Floods in Sudan 2024

The rainy season in both the Western Sahel and Sudan spans from May/June to September and is vital for agriculture and water resources, but also leads to flooding on a regular basis (Adefisan, 2018; Balogun et al. 2019; Balogun et al. 2021; Balogun et al. 2022; UN Floods). In 2024, as in 2022 (WWA, 2022), the season was marked by a northward shift of the Intertropical Convergence Zone (ITCZ) in combination with intensified monsoon winds, bringing substantial moisture to the region which led to the heavy rainfall across the whole region (e.g. Gimeno et al. 2016). For the Eastern part of the region, in particular Sudan, the Tropical Easterly Jet (TEJ) and easterly waves further bolstered moisture transport and atmospheric instability, creating conditions ripe for frequent, intense storms.

As a result of this combination of atmospheric conditions, the 2024 season in Sudan was marked by an unprecedented rainfall event from late July to late August. This was characterised by extraordinary precipitation and widespread flooding across typically wet and dry regions, surpassing historical averages, and causing significant damage to infrastructure, livelihoods, and ecosystems.

On August 6, Abu Hamad, a typically arid region in northern Sudan, received 142 mm of rainfall, nearly three times its previous record set in 1950. On August 9, Shendi received 126.2 mm surpassing records from 1998. These rainfall amounts caused elevated water levels, resulting in prolonged flooding in valleys and streams. This event underscores Sudan's growing vulnerability to climate change due to its dependence on rainfed agriculture and low adaptive capacity (Siddig et al. 2019).

The impact of these events was devastating. By September 4, 2024, the UN Office for the Coordination of Humanitarian Affairs (UN OCHA) reported about 491,100 people (or 88,600 families) affected by the flooding across 63 localities in 15 states, with approximately 143,200 people displaced (UN OCHA, 2024). The most affected states were North Darfur, Red Sea, South Darfur, and River Nile. Additionally, the UN OCHA reported that 35,518 homes were destroyed and 44,993 damaged.
The risk of disease outbreaks rose significantly due to the stagnant floodwaters. As reported by UN OCHA, 2024, The Sudan Federal Ministry of Health declared a cholera outbreak on August 12, 2024, following initial cases on July 22. By September 1, approximately 2,900 cholera cases had been

reported, resulting in 112 deaths (a 3.9% fatality rate) across Kassala, Gedaref, River Nile, Aj Jazirah, and Khartoum.

This calamity worsened existing challenges from ongoing conflicts, poverty, and food insecurity, greatly straining vulnerable communities. Critical infrastructure including roads, bridges, and dams in northern regions suffered substantial damage, disrupting transportation, communication, and access to essential services.

1.2 Extreme precipitation in Sudan and wider East Africa

Evidence increasingly links climate change to increased precipitation and severe flood events, as seen in West Africa's catastrophic 2022 floods. Enhanced rainfall and altered seasonal patterns have escalated urban flood impacts since 2007 (Adelekan 2015). By contrast, East Africa is currently grappling with an unprecedented drought crisis due to five successive failed rainy seasons (Busker et al. 2023). This illustrates the complex and varied impact of climate change across the African continent, affecting regions through both extreme flooding and prolonged droughts.
In Sudan, extreme rainfall events are typically characterised by intense precipitation, often resulting in severe flooding with significant environmental and socio-economic consequences. These events are largely driven by specific weather conditions, such as a warm equatorial Indian Ocean, a strong summer monsoon over Africa and India, and the northward displacement of the ITCZ (Williams and Nottage 2006).

To our knowledge, no attribution studies currently exist for heavy rainfall in the Eastern Sahel region . Chapter 11 of Working Group 1 of the IPCC reports that there is no detected or attributed change in such extremes due to human influence, resulting directly from a lack of evidence (Seneviratne et al., 2021). A study on this event should therefore offer tremendous value to understanding of risk in the region.

1.3 Event Definition

In Sudan, the impacted areas were affected by persistent rainfall that occurred between June and August. To reflect this, we study the wettest 30-day period over the study region (outlined in red in Figure 3) between June and August. We denote this seasonal maximum of 30-day rainfall as RX30day. The decision to analyse this specific region and temporal period was based on availability of data and the importance of capturing the most significant impacts within the region; the spatial extent covers the most impacted parts of the Nile and Bar el Ghazal river basins (Nile Basin initiative, n.d.). The regions to the east of the study region, which also experienced very heavy rainfall, are mountainous and have a very different climatology to the study region and therefore were not included in this study.

In this report, we examine the influence of anthropogenic climate change by comparing the likelihood and intensity of similar RX30day events in the present climate with those in a climate 1.3°C cooler. Additionally, we extend this analysis into the future by assessing the impact of a further 0.7°C increase in global warming from present levels.

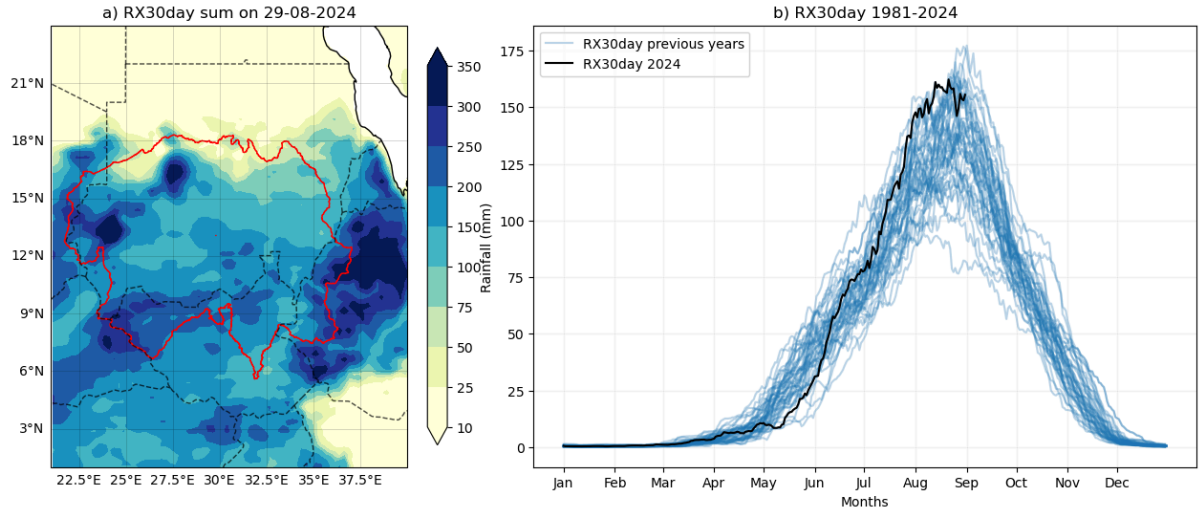

Fig. 3 a) Observed accumulated 30 day precipitation on 29 Aug 2024. The red highlight shows the area of study. b) 30-day cumulative rainfall over the study region from 1981-2024. Observations are taken from the CHIRPS dataset described in Section 2.1.

2 Data and methods

2.1 Observational data

In this analysis, we use a combination of data from local weather stations and gridded observations. The gridded product used to capture the spatial extent of the rainfall is the rainfall product developed by the UC Santa Barbara Climate Hazards Group called "Climate Hazards Group InfraRed Precipitation with Station data" (CHIRPS; Funk et al. 2015). Daily data are available at 0.25° resolution, from January 1981 until the end of August 2024. The product incorporates satellite imagery with in-situ station data. Daily rainfall observations for 17 stations from 1981-2021 in the study domain were made available by the Sudan Meteorological Authority (SMA). The station locations are shown in Figure 4. We use this data to evaluate the trends in CHIRPS over the region (see Section 3.1).

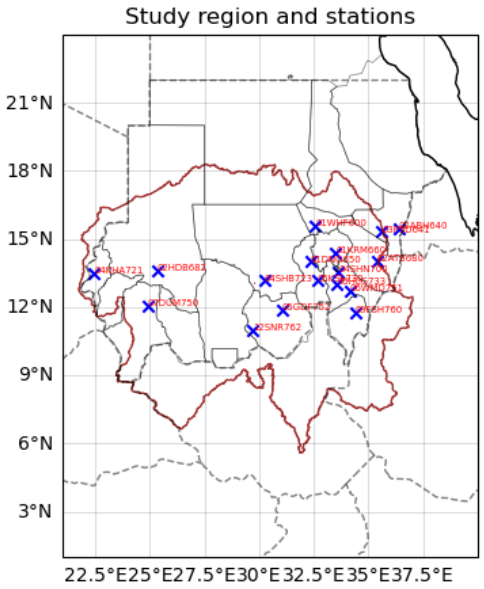

Figure 4: Locations of weather stations within the event domain used in this analysis.

As a measure of anthropogenic climate change we use the (low-pass filtered) global mean surface temperature (GMST), where GMST is taken from the National Aeronautics and Space Administration (NASA) Goddard Institute for Space Science (GISS) surface temperature analysis (GISTEMP, Hansen et al., 2010 and Lenssen et al. 2019).

2.2 Model and experiment descriptions

We use 2 multi-model ensembles from climate modelling experiments using different framings (Philip et al., 2020): coupled global circulation models and regional climate models.

1. Coordinated Regional Climate Downscaling Experiment (CORDEX)-Africa (0.44° resolution, AFR-44) multi-model ensemble (Nikulin et al., 2012), comprising of 17 simulations resulting from pairings of 9 Global Climate Models (GCMs) and 5 Regional Climate Models (RCMs). These simulations are composed of historical simulations up to 2005, and extended to the year 2100 using the RCP8.5 scenario.

2. CMIP6. This consists of simulations from 19 participating models with varying resolutions. For more details on CMIP6, please see Eyring et al., (2016). For all simulations, the period 1850 to 2015 is based on historical simulations, while the SSP5-8.5 scenario is used for the remainder of the 21st century.

2.3 Statistical methods

Methods for observational and model analysis and for model evaluation and synthesis are used according to the World Weather Attribution Protocol, described in Philip et al., (2020), with supporting details found in van Oldenborgh et al., (2021), Ciavarella et al., (2021) and here. The key

steps, presented in sections 3-6, are: (3) trend estimation from observations; (4) model evaluation; (5) multi-method multi-model attribution; and (6) synthesis of the attribution statement.

In this report we analyse time series of the wettest 30-day period (RX30day) during June-August each year in a region over Eastern Africa (figure 3). A nonstationary generalised extreme value distribution is used to model RX30day. For precipitation, the distribution is assumed to scale exponentially with the covariates, with the dispersion (the ratio between the standard deviation and the mean) remaining constant over time. The parameters of the statistical model are fitted using maximum likelihood estimation.

For each time series, we calculate the return period and intensity of the event under study for the 2024 GMST and for 1.3 C cooler GMST: this allows us to compare the climate of now and of the preindustrial past (1850-1900, based on the Global Warming Index), by calculating the probability ratio (PR; the factor-change in the event's probability) and change in intensity of the event.

The variable of interest , X, is assumed to follow a GEV distribution in which the location and scale parameters vary with GMST:

$$X \sim GEV(\mu, \sigma, \xi \mid \mu_0, \sigma_0, \alpha, T),$$

where X denotes the variable of interest, RX30day; T is the smoothed GMST; μ_0, σ_0 and ξ are the location, scale and shape parameters of the nonstationary distribution; and α is the trend due to GMST. As a result, the location and scale of the distribution have a different value in each year, determined by the GMST state of that year. Maximum likelihood estimation is used to estimate the model parameters, with

$$\mu = \mu_0 exp\left(\frac{\alpha T}{\mu_o}\right) \quad \text{and} \quad \sigma = \sigma_0 exp\left(\frac{\alpha T}{\mu_o}\right).$$

This formulation reflects the Clausius-Clapeyron relation, which implies that precipitation scales exponentially with temperature (Trenberth et.al., 2003, O'Gorman and Schneider 2009).

3 Observational analysis

3.1 Evaluation of gridded data against station data

Figure 5 shows the comparison of RX30day from individual meteorological stations with the nearest grid point of the CHIRPS data set. Overall the trends in RX30day from CHIRPS data are in agreement with those in the station data, although the magnitudes of the maxima are underestimated. Averaging the station totals and comparing with the area average of the study region leads to the same conclusion (Figure 6). RX30day is increasing over the region. These results give confidence in the usage of CHIRPS data to study this event. Comparison with other gridded data products, show very different behaviour to the station data. We thus only use CHIRPS for the observational analysis in this study.

This is not unexpected, as previous studies have also shown that many gridded global data products perform very poorly in the Sahel region (Kouakou et al., 2023).

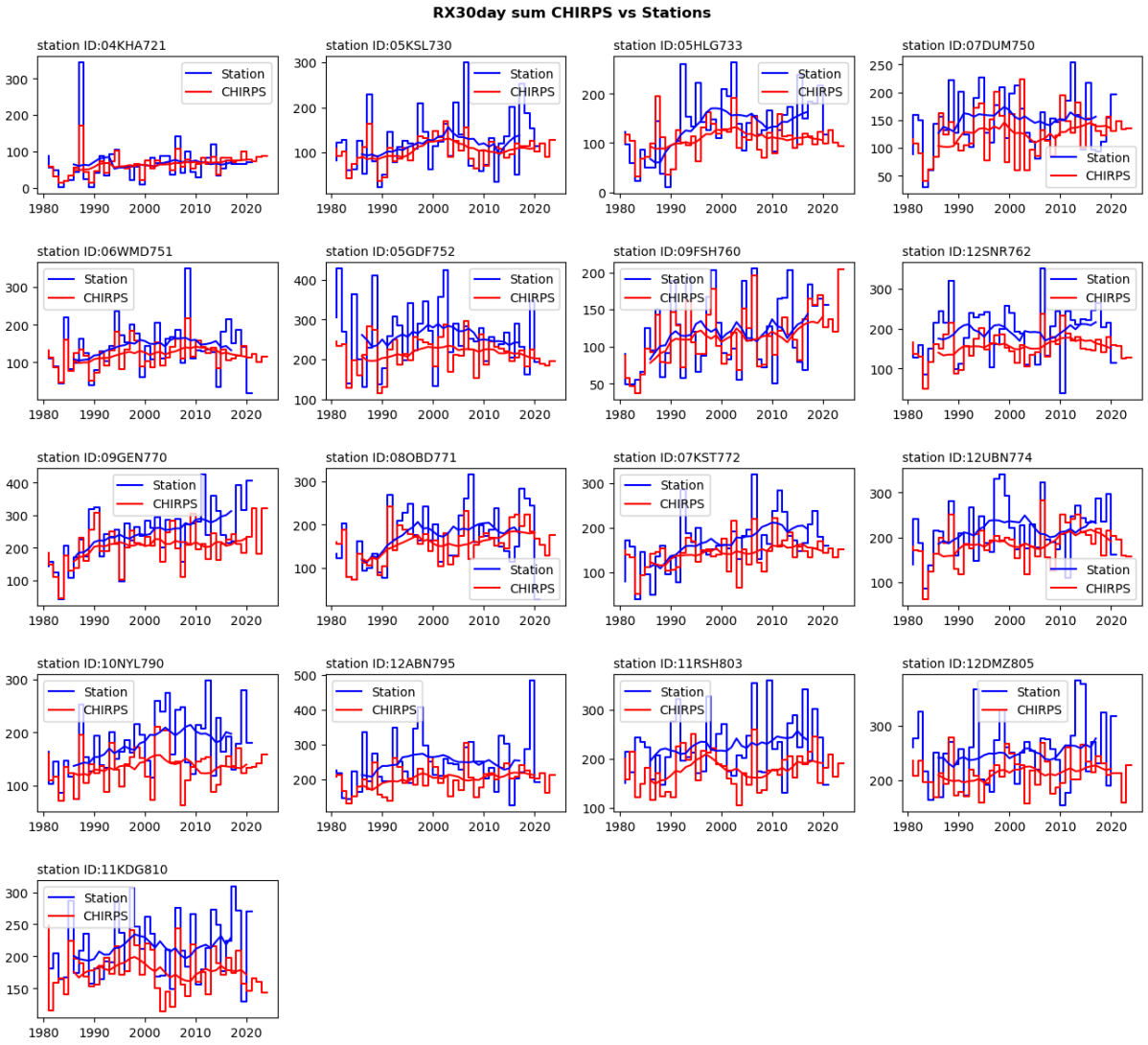

Figure 5: Time series of RX30day in individual weather stations (one per plot, blue line) and the closest grid point within the CHIRPS gridded data product (red line). The 10-year rolling mean is shown for each time series.

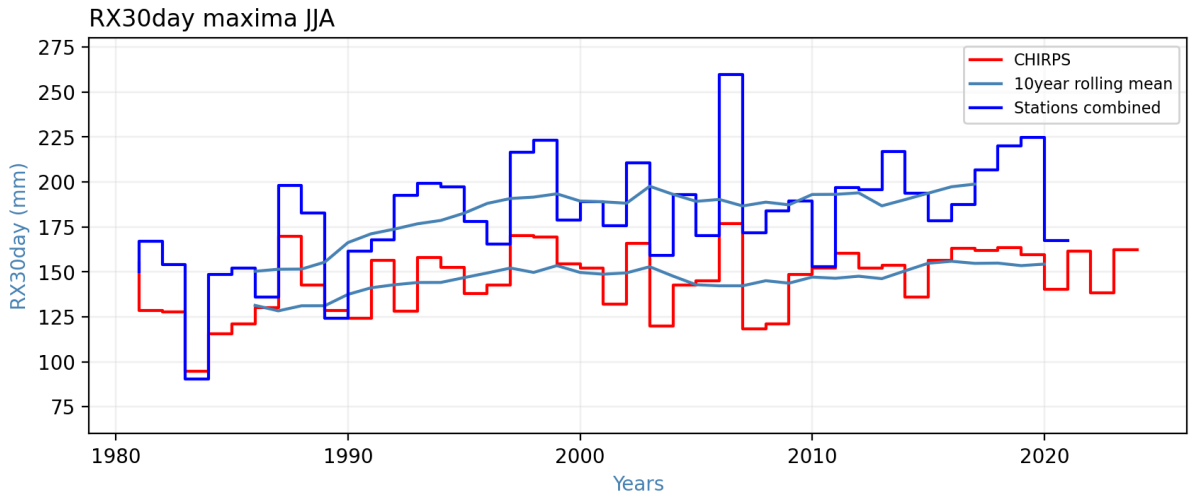

Figure 6. RX30day over the study domain from CHIRPS and available station data combined.

3.2 Evaluation of trends in gridded data

We use CHIRPS data to estimate the return periods and changes in both the probability and magnitude of the event across the study region. Figure 7 shows the trend fitting methods described in Philip et al. (2020) applied to the transient series of seasonal maximum 30-day average rainfall, for the study region. The 2024 event magnitude is 162.28 mm in the present day, this is estimated to be a relatively common event of approximately 1 in 3 years (uncertainty: 1.7 years to 15330 years). The intensity estimates indicate an 18% increase (uncertainty: -10.6% to 49.8%) in response to a 1.3C increase in GMST, and the probability ratio (the change in the likelihood of an event of this magnitude) is very large: 761 (uncertainty: 0.0168 to infinity).

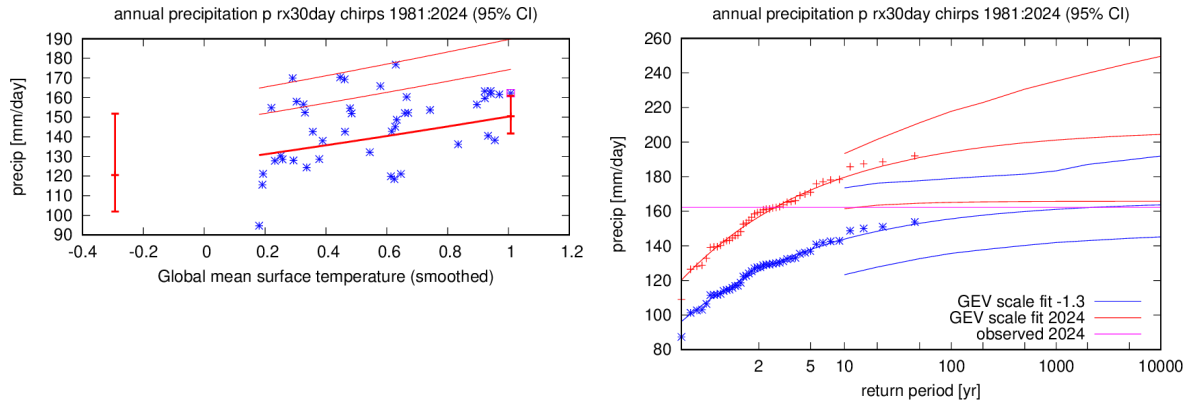

Figure 7. (Left) Response of RX30day to change in GMST, based on CHIRPS. The thick red line denotes the time-varying mean, and the thin red lines show the expected return level of a 1-in-6-year and 1-in-40-year event. The vertical red lines show the 95% confidence interval for the location parameter, for the current, 2024 climate and a hypothetical 1.3ºC cooler climate. The 2024 event is highlighted with the magenta box. (Right) Changes in return periods based on 2024 GMST (red lines) and 1.3°C lower GMST (blue lines). The markers show the data and the lines show the expected

values based on the statistical model, with 95% confidence bounds estimated by bootstrapping. The magenta line shows the magnitude of the 2024 event.

4 Model evaluation

In this section we show the results of the model evaluation for the assessed region. The climate models are evaluated against the observations in their ability to capture:

1. Spatial patterns (figure A1-A2): Models that do not match the observations in terms of the large-scale precipitation patterns are excluded.

2. Seasonal cycles (figure A3-A4): For this, we qualitatively compare the seasonal cycles based on model outputs against observations-based cycles. We discard the models that exhibit ill-defined peaks in their seasonal cycles. We also discard the model if the rainy season onset/termination varies significantly from the observations.

3. Parameters of the fitted statistical models (Table 1). We discard the model if the model and observation parameters ranges do not overlap.

The models are labelled as ‘good’,’reasonable’, or ’bad’ based on their performances in terms of the three criteria discussed above. A model is given an overall rating of ‘good’ if it is rated ‘good’ for all three characteristics. If there is at least one ‘reasonable’, then its overall rating will be ‘reasonable’ and ‘bad’ if there is at least one ‘bad’. An exception has been made for the spatial patterns, which were deemed to be either reasonable or bad for all models, in which case we still label the overall conclusion 'good' if all other characteristics are good, to identify those models that are better able to replicate other aspects of the distribution.

For each framing or model setup we also use models that only just pass the validation tests if we only have five models or less for that framing that perform well. The table shows the model evaluation results.

Table 1. Evaluation results of the climate models considered for attribution analysis of RX30day. For each model, the threshold for a 1-in-3 year event is shown, along with qualitative evaluations of the seasonal cycle and spatial pattern; the best estimates of the Dispersion and Shape parameters, with bootstrapped 95% confidence intervals in brackets; and the final conclusion is listed in the 'Conclusion' column. Rows are coloured according to the overall conclusion - green for 'good', yellow for 'reasonable' and red for 'bad'.

Model / Observations	Threshold 1 in 3 year event in mm	Seasonal cycle	Spatial pattern	Dispersion	Shape parameter	Conclusion
CHIRPS				0.127 (0.087... 0.18)	-0.42 (-1.1 ... -0.12)	
CanESM2_CCCma-CanRCM4	190.2	good	reasonable	0.100 (0.0800 ... 0.120)	-0.18 (-0.41 ... 0.0)	good
CanESM2_SMHI-RCA4	103.5	good	reasonable	0.140 (0.110 ... 0.160)	-0.020 (-0.23 ... 0.19)	good
CNRM-CM5_CLMcom-CCLM4-8-17	204.9	good	reasonable	0.110 (0.0900 ... 0.130)	-0.20 (-0.37 ... 0.0)	good

CNRM-CM5_SMHI-RCA4	115.4	good	reasonable	0.130 (0.110 ... 0.150)	-0.15 (-0.38 ... -0.020)	good
EC-EARTH_CLMcom-CCLM4-8-17	230.2	good	reasonable	0.180 (0.140 ... 0.220)	-0.34 (-0.62 ... -0.13)	bad (threshold high)
EC-EARTH_MPI-CSC-REMO2009	94.3	good	reasonable	0.290 (0.240 ... 0.330)	-0.30 (-0.56 ... -0.14)	bad
EC-EARTH_KNMI-RACMO22T	243.8	good	reasonable	0.200 (0.160 ... 0.220)	-0.26 (-0.49 ... -0.12)	bad (threshold high)
EC-EARTH_SMHI-RCA4	159	good	reasonable	0.180 (0.140 ... 0.210)	-0.21 (-0.38 ... -0.020)	good
IPSL-CM5A-LR_SMHI-RCA4	86.6	good	reasonable	0.160 (0.130 ... 0.180)	0.040 (-0.13 ... 0.24)	bad (threshold low)
MIROC5_SMHI-RCA4	135.8	good	reasonable	0.150 (0.120 ... 0.170)	-0.12 (-0.28 ... 0.020)	good
HadGEM2-ES_CLMcom-CCLM4-8-17	211.9	good	reasonable	0.140 (0.100 ... 0.170)	-0.48 (-0.65 ... -0.25)	good
HadGEM2-ES_SMHI-RCA4 ()	131.9	good	reasonable	0.140 (0.110 ... 0.160)	-0.12 (-0.25 ... 0.030)	good
MPI-ESM-LR_CLMcom-CCLM4-8-17	196.4	good	reasonable	0.2 (0.15 ...0.24)	-0.27 (-0.42 ...-0.13)	bad
MPI-ESM-LR_MPI-CSC-REMO2009	95.4	good	reasonable	0.250 (0.200 ... 0.280)	0.020 (-0.14 ... 0.18)	bad
MPI-ESM-LR_SMHI-RCA4	141.7	good	reasonable	0.150 (0.120 ... 0.170)	-0.24 (-0.42 ... 0.0)	good
NorESM1-M_SMHI-RCA4	115.8	good	reasonable	0.150 (0.120 ... 0.180)	0.020 (-0.12 ... 0.19)	good
NOAA-GFDL_SMHI-RCA4	112.1	good	reasonable	0.180 (0.140 ... 0.220)	-0.29 (-0.68 ... -0.12)	good
ACCESS-CM2	116.2	good	reasonable	0.260 (0.220 ... 0.300)	0.060 (-0.12 ... 0.25)	bad
ACCESS-ESM1-5	264.6	good	reasonable	0.180 (0.150 ... 0.220)	-0.25 (-0.68 ... -0.11)	reasonable
CanESM5	161.5	good	reasonable	0.200 (0.160 ... 0.230)	-0.24 (-0.47 ... -0.020)	reasonable
CMCC-ESM2	150.1	good	reasonable	0.110 (0.0800 ... 0.120)	-0.050 (-0.26 ... 0.17)	reasonable
CNRM-CM6-1-HR	34.1	bad	bad	0.450 (0.340 ... 0.520)	0.13 (-0.050 ... 0.37)	bad
CNRM-CM6-1	31.4	bad	bad	0.660 (0.540 ... 0.760)	0.25 (0.050 ... 0.44)	bad
EC-Earth3	149.4	good	reasonable	0.150 (0.120 ... 0.190)	-0.040 (-0.26 ... 0.24)	reasonable
EC-Earth3-Veg	142.1	good	reasonable	0.190 (0.150 ... 0.220)	-0.28 (-0.53 ... -0.090)	reasonable
EC-Earth3-Veg-LR	124.5	good	reasonable	0.150 (0.120 ... 0.170)	-0.070 (-0.27 ... 0.11)	reasonable
FGOALS-g3	59.6	reasonable	bad	0.210 (0.170 ... 0.240)	0.13 (-0.030 ... 0.29)	bad
INM-CM4-8	133.3	good	reasonable	0.140 (0.100 ... 0.170)	-0.080 (-0.26 ... 0.17)	reasonable
INM-CM5-0	116.6	good	reasonable	0.130 (0.0900 ... 0.150)	0.050 (-0.14 ... 0.35)	reasonable
MIROC6	223	good	reasonable	0.150 (0.130 ... 0.190)	-0.18 (-0.71 ... -0.040)	good
MPI-ESM1-2-HR	146.7	good	reasonable	0.270 (0.220 ... 0.320)	-0.50 (-0.79 ... -0.27)	bad
MPI-ESM1-2-LR	150.4	good	reasonable	0.220 (0.170 ... 0.260)	-0.12 (-0.33 ... 0.030)	reasonable
MRI-ESM2-0	145.5	good	bad	0.180 (0.150 ... 0.200)	-0.24 (-0.52 ... -0.070)	reasonable
NorESM2-LM	142.4	good	reasonable	0.220 (0.180 ... 0.240)	-0.070 (-0.31 ... 0.10)	reasonable
NorESM2-MM	156.5	good	reasonable	0.170 (0.130 ... 0.200)	-0.33 (-0.50 ... -0.15)	good
TaiESM1	152.7	good	reasonable	0.100 (0.0700 ... 0.110)	0.070 (-0.11 ... 0.29)	bad

5 Multi-method multi-model attribution

This section shows Probability Ratios and relative changes in intensity for models that passed model evaluation and also includes the values calculated from the fits with observations.

Table 2. Event magnitude, probability ratio and change in intensity for the 2024 observed RX30day for observational dataset and corresponding estimates for 3-year return level for each model that passed the evaluation tests. (a) from pre-industrial climate to the present and (b) from the present to 2℃ above pre-industrial climate.

Model / Observations	**2024 event /Threshold for return period 3 yr**	**(a) Pre-industrial (1.3C cooler) climate to present 2024 climate**		**(b) Present 2024 climate to future 0.7C warmer world**	
		Probability ratio PR [-]	**Change in intensity ΔI [%]**	**Probability ratio PR [-]**	**Change in intensity ΔI [%]**
CHIRPS	162 mm	761 (0.017 ... 7.1e+16)	18 (-11 ... 50)		
CanESM2_CCCma-CanRCM4	190.19 mm	7.8 (4.2 ... 23)	15 (8.5 ... 21)	1.5 (1.4 ... 1.8)	5.4 (3.8 ... 7.0)
CanESM2_SMHI-RCA4	103.5 mm	2.1 (1.1 ... 3.9)	11 (0.87 ... 20)	1.1 (0.95 ... 1.3)	1.9 (-0.67 ... 4.8)
CNRM-CM5_CLMcom-CCLM4-8-17	204.91 mm	1.0 (0.36 ... 2.7)	0.27 (-9.9 ... 10)	0.83 (0.60 ... 1.1)	-2.1 (-5.1 ... 1.5)
CNRM-CM5_SMHI-RCA4	115.37 mm	1.1 (0.42 ... 2.7)	0.91 (-9.3 ... 14)	0.99 (0.72 ... 1.2)	-0.20 (-3.5 ... 2.9)
EC-EARTH_SMHI-RCA4	158.95 mm	2.8 (0.74 ... 8.6)	13 (-2.8 ... 31)	1.0 (0.73 ... 1.2)	0.090 (-4.0 ... 3.6)
MIROC5_SMHI-RCA4	135.81 mm	2.2 (0.58 ... 7.7)	10 (-5.5 ... 27)	1.4 (1.1 ... 1.6)	5.6 (1.7 ... 9.1)
HadGEM2-ES_CLMcom-CCLM4-8-17	211.91 mm	7.0 (2.9 ... 22)	11 (3.7 ... 17)	1.3 (1.0 ... 1.4)	2.8 (0.34 ... 5.0)
HadGEM2-ES_SMHI-RCA4	131.87 mm	1.9 (0.97 ... 3.6)	7.7 (-0.28 ... 16)	1.1 (0.96 ... 1.3)	1.52 (-0.49... 3.3)
MPI-ESM-LR_SMHI-RCA4	141.71 mm	0.86 (0.44 ... 1.8)	-2.0 (-11 ... 8.6)	0.86 (0.62 ... 1.1)	-1.9 (-4.7 ... 1.2)
NorESM1-M_SMHI-RCA4	115.81 mm	1.7 (0.61 ... 4.4)	8.4 (-7.0 ... 24)	1.1 (0.93 ... 1.3)	2.1 (-1.2 ... 5.3)
NOAA-GFDL_SMHI-RCA4	112.08 mm	0.57 (0.093 ... 1.3)	-11 (-29 ... 7.4)	0.53 (0.29 ... 0.77)	-7.92(-11.7 ... -4.1)
ACCESS-ESM1-5	264.55 mm	2.3 (0.65 ... 5.6)	11 (-4.2 ... 25)	1.2 (1.4 ... 0.93)	3.0 (-1.2 ... 6.3)
CanESM5	161.53 mm	2.1 (1.0 ... 4.2)	11 (0.34 ... 23)	1.4 (1.6 ... 1.2)	5.9 (3.7 ... 8.6)
CMCC-ESM2	150.09 mm	3.7 (1.5 ... 18)	13 (3.3 ... 23)	1.4 (1.7 ... 1.1)	4.0 (1.4 ... 7.0)
EC-Earth3	149.4 mm	8.4 (3.4 ... 30)	28 (17 ... 41)	1.7 (2.1 ... 1.5)	10 (7.6 ... 13)
EC-Earth3-Veg	142.08 mm	3.4 (1.0 ... 14)	14 (0.0 ... 31)	1.5 (1.7 ... 1.3)	7.6 (3.2 ... 12)
EC-Earth3-Veg-LR	124.54 mm	7.4 (2.4 ... 2.4e+2)	25 (10 ... 44)	1.65 (2.08 ... 1.37)	9.1 (5.5 ... 13)
INM-CM4-8	133.25 mm	2.0 (0.76 ... 6.1)	9.1 (-3.1 ... 24)	1.8 (2.2 ... 1.5)	9.4 (5.7 ... 13)
INM-CM5-0	116.62 mm	1.5 (0.48 ... 4.2)	5.4 (-10 ... 23)	1.6 (1.9 ... 1.3)	7.11 (3.6 ... 10.25)
MIROC6	223 mm	17 (1.9 ... 1.0e+4)	27 (7.0 ... 54)	2.0 (2.4 ... 1.7)	13 (9.8 ... 18)
MPI-ESM1-2-LR	150.39 mm	2.0 (0.59 ... 8.5)	13 (-7.7 ... 43)	1.6 (1.8 ... 1.3)	10 (4.9 ... 16)

NorESM2-LM	142.44 mm	1.2 (0.44 ... 3.1)	3.3 (-14 ... 26)	0.99 (1.3 ... 0.71)	-0.13 (-5.5 ... 5.5)
NorESM2-MM	156.5 mm	0.60 (0.27 ... 1.2)	-8.8 (-19 ... 2.7)	0.73 (0.95 ... 0.44)	-3.9 (-7.6 ... -0.78)

6 Hazard synthesis

We evaluate the influence of anthropogenic climate change on the 2024 RX30day event by calculating the probability ratio as well as the change in intensity using observations and climate models. Models which do not pass the evaluation described above are excluded from the analysis. The aim is to synthesise results from models that pass the evaluation along with the observations-based products, to give an overarching attribution statement.

Figures 8 and 9 show the changes in probability and intensity for the observations (blue) and models (red) between the past and current, and current and future climates, respectively. The results are also shown in Table 2. A term to account for intermodel spread is added (in quadrature) to the natural variability of the models. This is shown in the figures as white boxes around the light red bars. The dark red bar shows the model average, consisting of a weighted mean using the (uncorrelated) uncertainties due to natural variability plus the term representing intermodel spread (i.e., the inverse square of the white bars).

Observation-based products and models are combined into a single result in two ways. Firstly, we neglect common model uncertainties beyond the intermodel spread that is depicted by the model average, and compute the weighted average of models (dark red bar) and observations (dark blue bar): this is indicated by the magenta bar. Since, due to common model uncertainties, model uncertainty can be larger than the intermodel spread, secondly, we also show the more conservative estimate of an unweighted, direct average of observations (dark red bar) and models (dark blue bar) contributing 50% each, indicated by the white box around the magenta bar in the synthesis figures.

As expected, the probability ratio in observations show large uncertainties when compared with models: as precipitation is generally highly variable, the relatively short time series implies uncertainties will be large. The best estimate of PR for observations is however clearly above 1, as expected in a warmer atmosphere that can hold more moisture, pointing towards higher precipitation values and more frequent extreme precipitation events. The combined results for the observations and models suggest a doubling in the likelihood of similar events and an increase in intensity of about 10% (Table 3). These best estimates and the uncertainty are clearly pointing towards a trend towards more frequent extremes and more severe precipitation. This is the same order of magnitude as what is expected from the Clausius-Clapeyron relation, even though that is related to shorter time scales. Although the uncertainty is large, the majority of the models also point towards a trend toward more extreme precipitation events. Therefore we only communicate the best estimates.

When assessing the change in likelihood and intensity for this event in a 0.7°C warmer climate compared to today, we find that almost all models show an increase in likelihood and intensity, but it is relatively small with a factor change in likelihood of 1.20 and an increase in intensity of 3.5% for

the best estimates. The direction of change is however again in line with changes between the past and current climate.

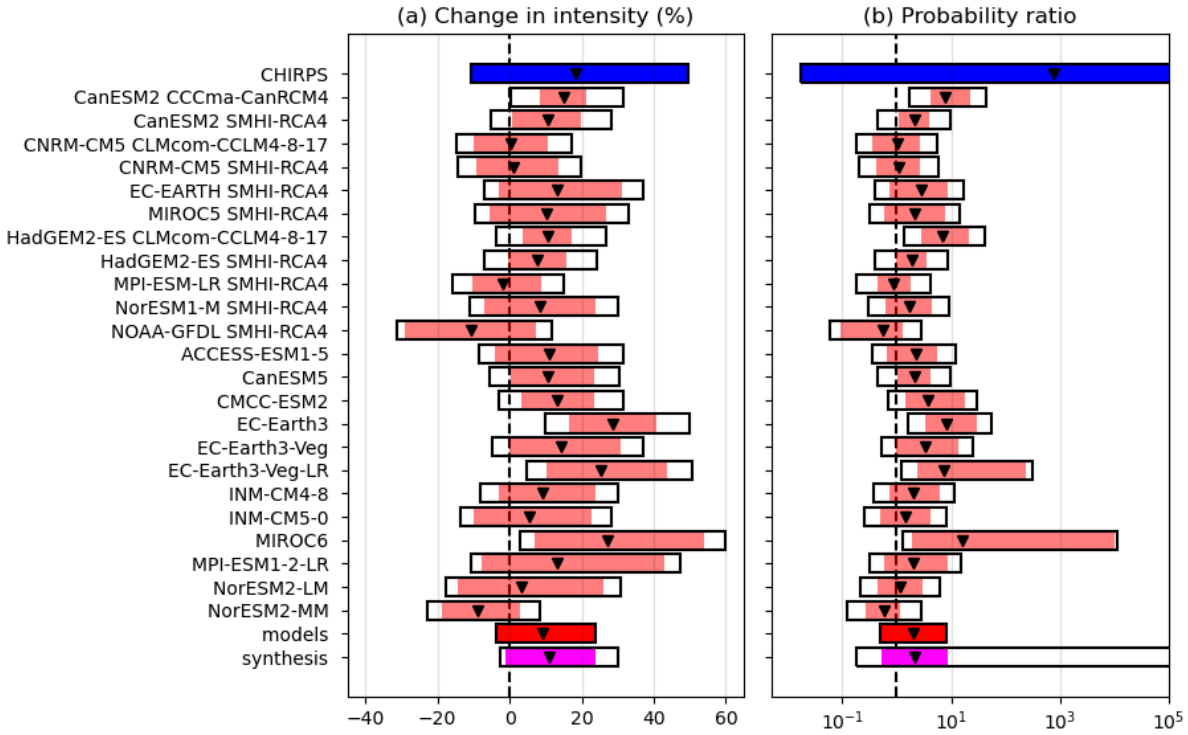

Figure 8: Synthesis of (a) intensity change and (b) probability ratios when comparing RX30day over the study region with a 1.3C cooler climate. The x-axis has been truncated to show detail: the upper bound for CHIRPS is 7.1e16, and for the unweighted synthesis is 3.8e9.

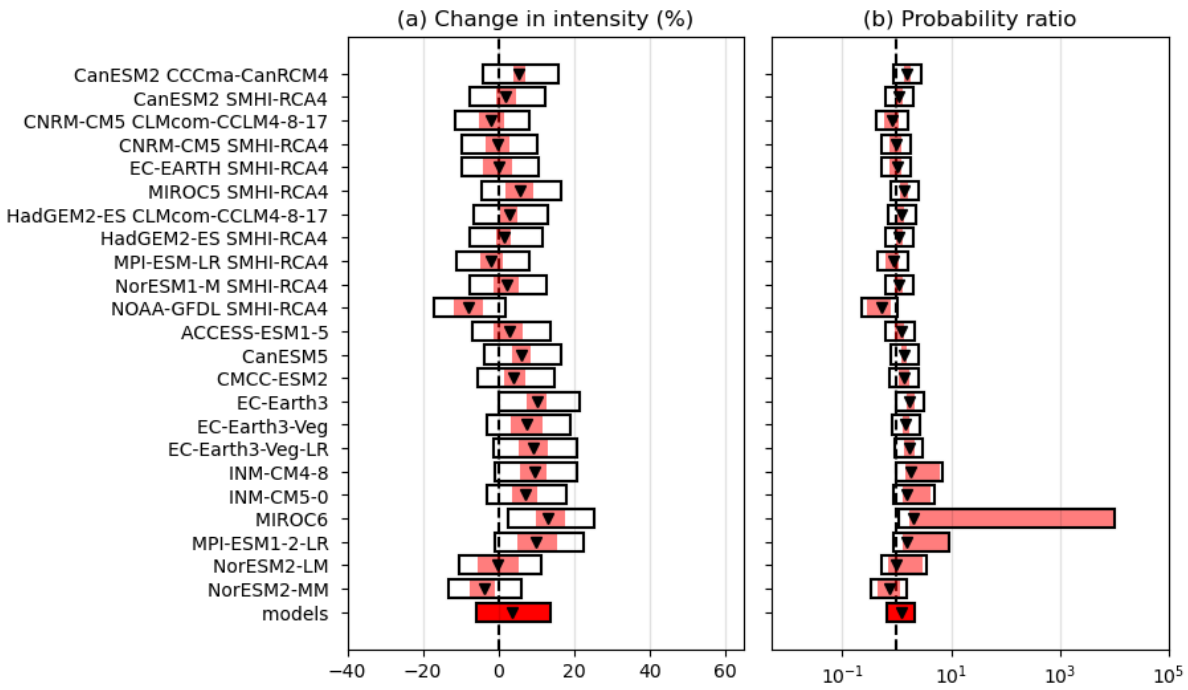

Figure 9: Synthesis of intensity change (left) and probability ratios (right), when comparing RX30day event over the study region after a further 0.7°C of warming (a total of 2°C since pre-industrial)

Table 3: Summary of results for Rx30day, presented in Figs 5 and 6

Data		GMST	
		Probability ratio (95% CI)	**Intensity change (%) (95% CI)**
Observations	**Past- Present**	761 (0.0168 .. 0.707E+17)	18.2 (-10.6 … 49.6)
Models		2.06 (0.504 … 8.44)	9.28 (-3.64 … 23.9)
Synthesis		2.11 (0.519 … 8.66)	10.9 (-1.10 … 24.0)
Models only	**Present- Future**	1.20 (0.675 … 2.12)	3.52 (-5.77 … 13.7)

7 Vulnerability and exposure

The 2024 floods in Sudan, triggered by the heaviest rainfall since 2019, have intensified a pre-existing humanitarian crisis. The nearly nation-wide flooding (see Figure 10) began in June with the onset of the rainy season and was compounded by the partial collapse of the Arba'at Dam on August 25, which unleashed flash floods, further damaging critical infrastructure, including roads, water system, and telecommunications (ECHO, 2024, 30 Aug; OCHA, 2024, 27 Aug). The most severely affected states include North Darfur, Red Sea, Northern, South Darfur, and River Nile, with significant but still undetermined impacts in Khartoum, Gezira, and Kordofan (OCHA, 2024, 5 Sept; Al Jazeera Centre for Public Liberties & Human Rights, 2024).

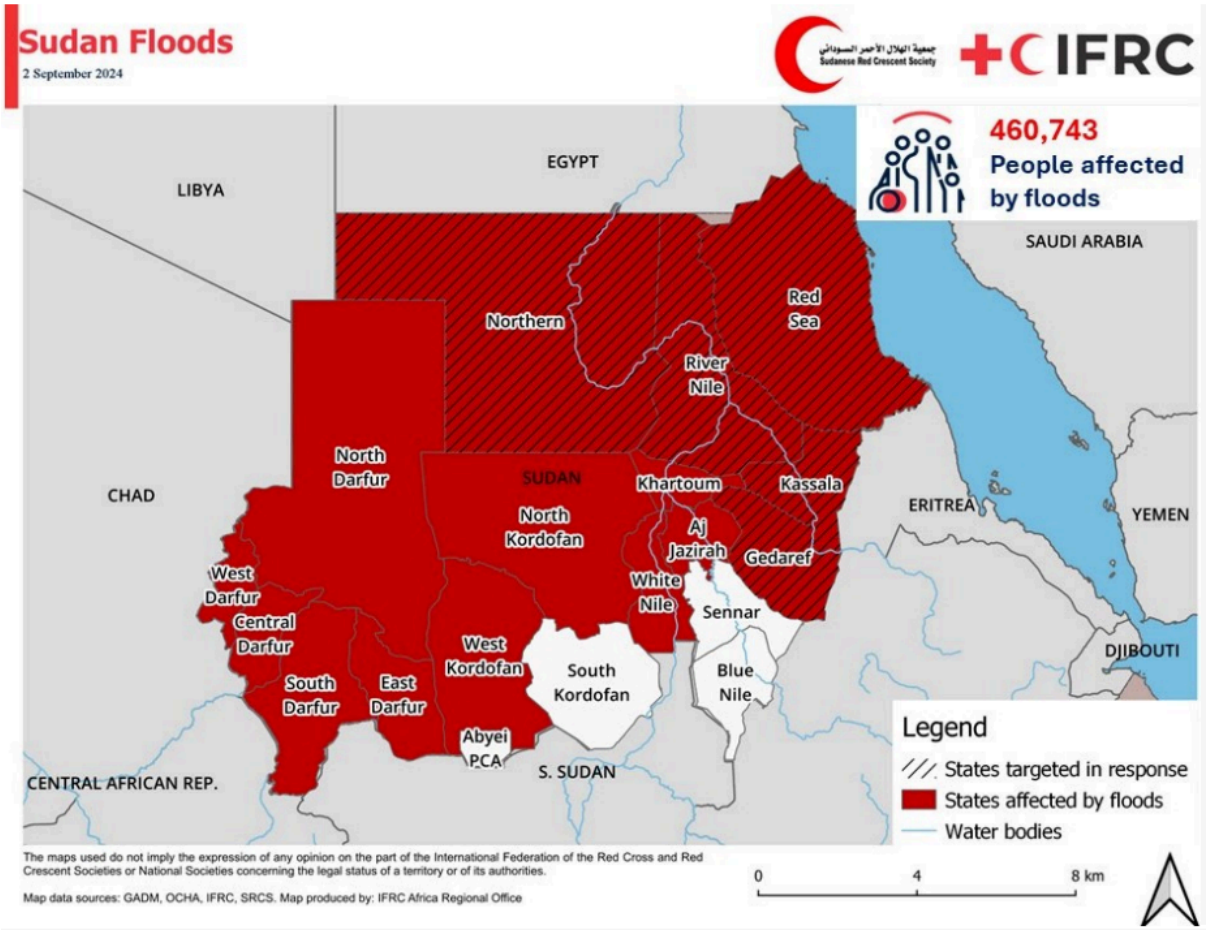

Figure 10. *Map of Sudan, indicating the states affected by the 2024 floods including the worst-affected which the emergency response is targeting. Source: IFRC (2024).*

The flooding coincides with numerous compounding factors, including ongoing conflict, large-scale displacement, deteriorating public health, acute food insecurity, and a deepening cost of living crisis. The conflict, which has continued for over 500 days, has led to widespread displacement, with millions of internally displaced persons (IDPs) particularly vulnerable to flooding due to their temporary shelters and limited access to basic services. Flooding in IDP camps has resulted in further displacement and loss of shelter (OCHA, 2024, 1 Sept).

Flooding in 2024 has worsened public health risks, particularly through a cholera outbreak in Sudan, affecting over 2,900 people and causing 112 deaths across five states (OCHA, 2024, 5 Sept). Floodwaters have also deepened famine conditions, with North Darfur, particularly the Zamzam IDP camp near Al Fasher, declaring a global famine and agricultural losses undermining livelihoods (OCHA, 2024, 25 Aug). In West and Central Africa, floods have destroyed critical infrastructure, increasing the spread of waterborne diseases, including cholera, which has claimed over 350 lives in Nigeria (OCHA, 2024, 15 Oct). Chad and Nigeria, already facing multidimensional crises linked to conflict and climate shocks, have been severely affected, with millions displaced and livelihoods disrupted (USAID, 2024, 18 Sep; OCHA, 2024, 9 Oct). Chad, hosting over one million refugees, faces increased strain (USAID, 2024, 18 Sep).

Crucially, the flooding in Nigeria hit at nearly the identical place and time as the devastating floods in 2022. A report by UNDP (2023) highlighted that roughly half (52.5%) and 41.5% of the urban and

rural populations, respectively had recovered on average, with states like Kogi and Delta indicating rates as low as 21.5 and 25.3%, and Anambra as high as 69.2%. The ability to recover has been linked to resuming work (16.3%), recovering from food scarcity (15.2%), and rehabilitating damaged infrastructure (11.7%) (Ibid.).

Rapid growth in urban and informal settlements, against the backdrop of inadequate urban planning and governance, means that vulnerable people become at-risk for impacts from various hazards because they settle in areas which expose them to impacts from landslides, floods, sea-level rise, and storm surge (IPCC, 2022). The combination of these factors has created a complex and interlinked crisis, making the 2024 floods particularly devastating and challenging to manage. While the flooding is widespread, the vulnerability and exposure analysis focuses on Sudan, Nigeria, and Chad.

7.1 Conflict and displacement

Ongoing conflicts and widespread displacement in Sudan, Nigeria, and Chad have amplified flood risks, intensifying vulnerabilities. The intersection of conflict and climate change, driven by migration pressures, maladaptation, and weak governance, further exacerbates competition for resources and creates opportunities for instability (Tarif, 2022).

The ongoing conflict in Sudan has significantly deteriorated infrastructure and basic services, exacerbating the impact of the 2024 floods and heightening displacement risks. The conflict has damaged essential infrastructure, including water supplies, roads, and telecommunication networks, complicating flood response efforts (IOM, 2024, 29 Aug). The destruction of vital facilities has left communities more vulnerable to flooding, as weakened infrastructure cannot support evacuation or provide adequate shelter. The Arba'at Dam's collapse exemplifies the compounded risk, as it follows substantial flooding that has already displaced over 136,000 people (IOM, 2024, 29 Aug). Those living on the dam's western side, many of whom were already displaced due to conflict, faced heightened vulnerabilities when floodwaters surged.

Urban centres, including Al Fasher in North Darfur, have experienced severe impacts from both conflict and floods. The area's internal displacement camps, such as Zamzam and Abu Shouk, saw extensive damage to shelters and sanitation facilities due to flooding (OCHA, 2024, 1 Sept). These urban areas, often characterised by makeshift shelters and inadequate drainage, lack the resilience needed to withstand such climatic events. Limited urban planning and the collapse of governance have left cities with inadequate drainage systems, increasing flood risk and contributing to poor living conditions for internally displaced persons (IDPs).

Public health challenges have also intensified amid the crisis. The displacement crisis has contributed to overcrowded camps with poor sanitation, creating conditions ripe for disease outbreaks. The 2024 floods have worsened the spread of waterborne diseases, including a cholera epidemic (OCHA, 2024, 5 Sept). Between July and September, nearly 5,700 cholera cases, with a 3.9% case fatality rate, were reported, demonstrating the compounded health risks of displacement and floods (Abdelrheem, 2024).

In total, the floods affected over 172,520 individuals, with 41% of those already displaced due to conflict (DTM, 2024, 27 Aug). On 22 August, the Sudan refugee situation in Libya was declared a level two emergency, enabling increased resources and aid delivery through key entry points like

Alkufra and Tobruk (UNHRC, 2024). Figure 11 reveals that displacement due to floods is concentrated in states like River Nile (57,925), North Darfur (34,270), Northern (22,860), West Darfur (20,025), and Red Sea (19,690) (DTM, 2024, 27 Aug). As Sudan's infrastructure continues to erode under conflict, the cycle of displacement and vulnerability deepens, particularly for those in flood-prone regions like Darfur and the River Nile states.

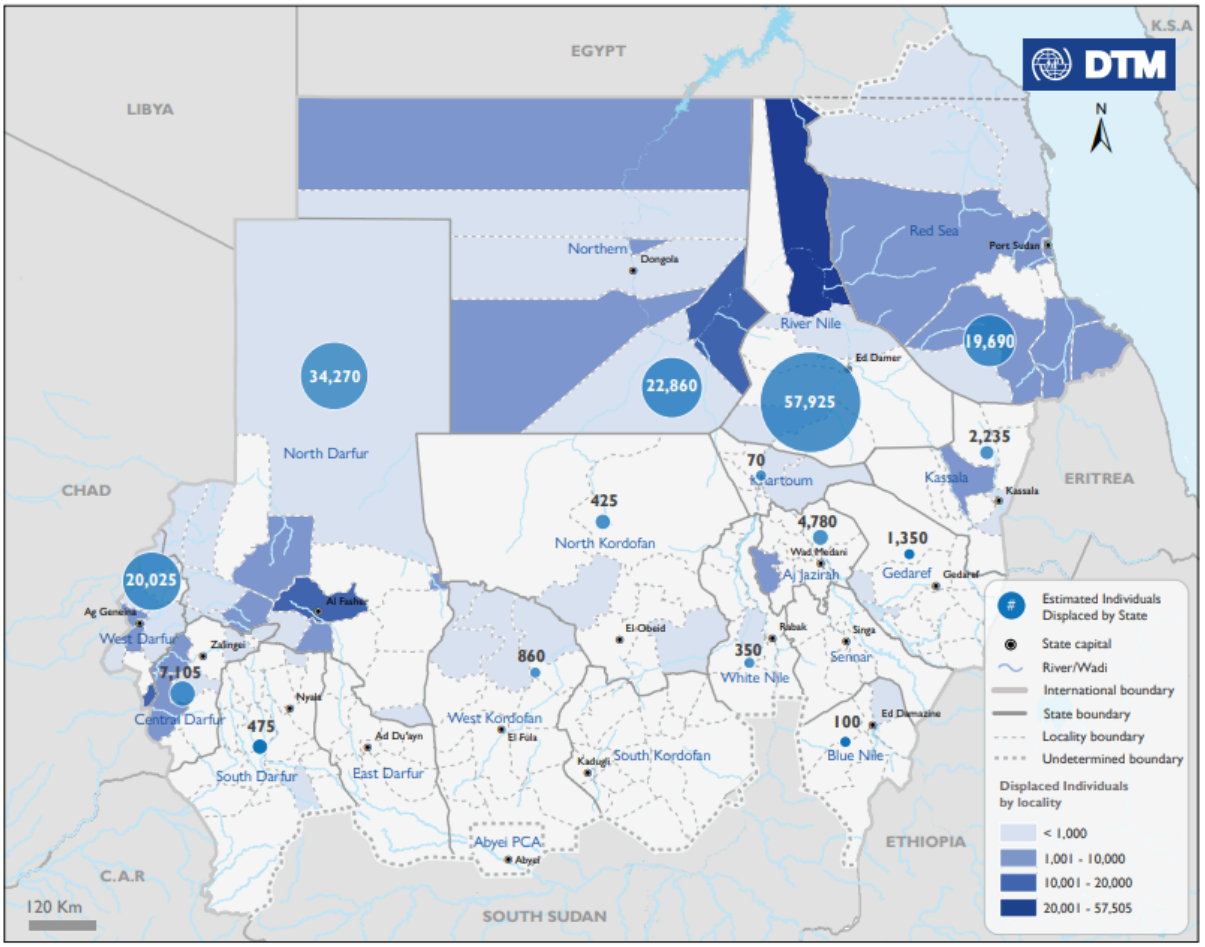

This map is for illustration purposes only. Names and boundaries on this map do not imply official endorsement or acceptance by IOM.

Map 1: Estimated Individuals Displaced by Floods Per State, 01 June - 4 September 2024

Figure 11. *Map showing estimated number of individuals by floods per state between 1 June and 4 September. Source: DTM (2024, 4 Sept).*

The situation in Chad exceeds the catastrophic floods of 2022 – previously deemed the worst in a decade (IFRC, 2024). The areas surrounding Lake Chad and the Lower Niger basins are especially vulnerable to climate change impacts with national and local factors leading to varying cascading effects regionwide, including food insecurity and broader trade and mobility. Conflict in these regions is primarily natural resource-based and is worsened by the presence of armed groups (Vivekananda, Schilling, & Smith, 2014). Armed insurgencies in northeastern Nigeria, eastern Niger, and parts of Cameroon and Chad have increased security and diminished state presence in some areas hardest hit by flooding (Brechenmacher, 2019). Armed groups like Boko Haram recruit from communities whose livelihoods are impacted by factors including extreme weather; and local militias can escalate farmer-herder conflicts, thus eroding community resilience and increasing vulnerability (Ibid.).

Chad is one of the countries with the highest numbers of IDPs and refugees globally (UNHCR, 2022). The Internal Displacement Monitoring Centre (IDMC) tracks estimates of internal displacement caused by conflict and climate-related events. Between 2008 to 2023, 35 reported flood events displaced ~985,000 people in Chad (IDMC, 2023a), while 101 reported flood events resulted in the displacement of ~8.7 million people in Nigeria (IDMC, 2023b). Between 2008 and 2023, conflict accounted for 452,000 IDPs in Chad and 3.3 million IDPs in Nigeria (IDMC, 2023a; IDMC, 2023b). It is anticipated that displacement in already-vulnerable countries will rise as the impacts of climate change continue to intensify (IPCC WGII, chapter 16, 2022; IDMC, 2022).

7.2 Water governance and adaptation

The 2024 floods in Sudan have exposed challenges in water governance and adaptation, particularly regarding shared water resources like the Nile. The Nile Basin Initiative (NBI) promotes basin-wide cooperation, yet Sudan's commitments under the 1959 Nile Waters Agreement with Egypt complicate this. Limited data sharing and political tensions hinder comprehensive flood management, affecting early warning systems and the effectiveness of transboundary water governance (Knaepen & Byiers, 2017). On 13 October, 2024, the Nile River Basin Cooperative Framework Agreement (CFA) entered into force, after ratification by six upstream countries: Ethiopia, Rwanda, Burundi, Tanzania, and South Sudan (Nile Basin Initiative, n.d.; The New Arab, 2024). The CFA is a legal framework designed to manage the sustainable use and development of the Nile's water resources, with the aim to rectify historical imbalances, ensure equitable water use, and establish the Nile River Basin Commission for regional cooperation (Nile Basin Initiative, n.d.). However, Sudan and Egypt oppose the agreement, citing concerns over water security and international law, especially with Egypt's heavy reliance on the Nile and Ethiopia's development of the Grand Ethiopian Renaissance Dam (The New Arab, 2024). The need for a better coordinated flood response among riparian countries is highlighted by the Blue Nile's seasonal flooding, exacerbated by water releases from upstream sources like Lake Victoria (OCHA, 2024, 29 Aug).

Water-health linkages have also become evident, as floodwaters exacerbate cholera outbreaks, notably in Red Sea State following the collapse of a spillway of the Arba'at Dam (UNHCR, 2024, 2 Sept; NEMA, 2024, 12 Sept). It is not yet clear if the collapse was a result of a design flaw, damage to the dam, or other reason. The map in Figure 12 illustrates the extensive flooding around Port Sudan, including significant inundation of built-up areas and damage to critical transportation routes. The dam, the primary freshwater source for Port Sudan, suffered damage after years without proper maintenance (Sio, 2024, 26 Aug). This collapse disrupted water supplies, intensifying the cholera crisis at a critical time (CNN, 2024, 28 Aug).

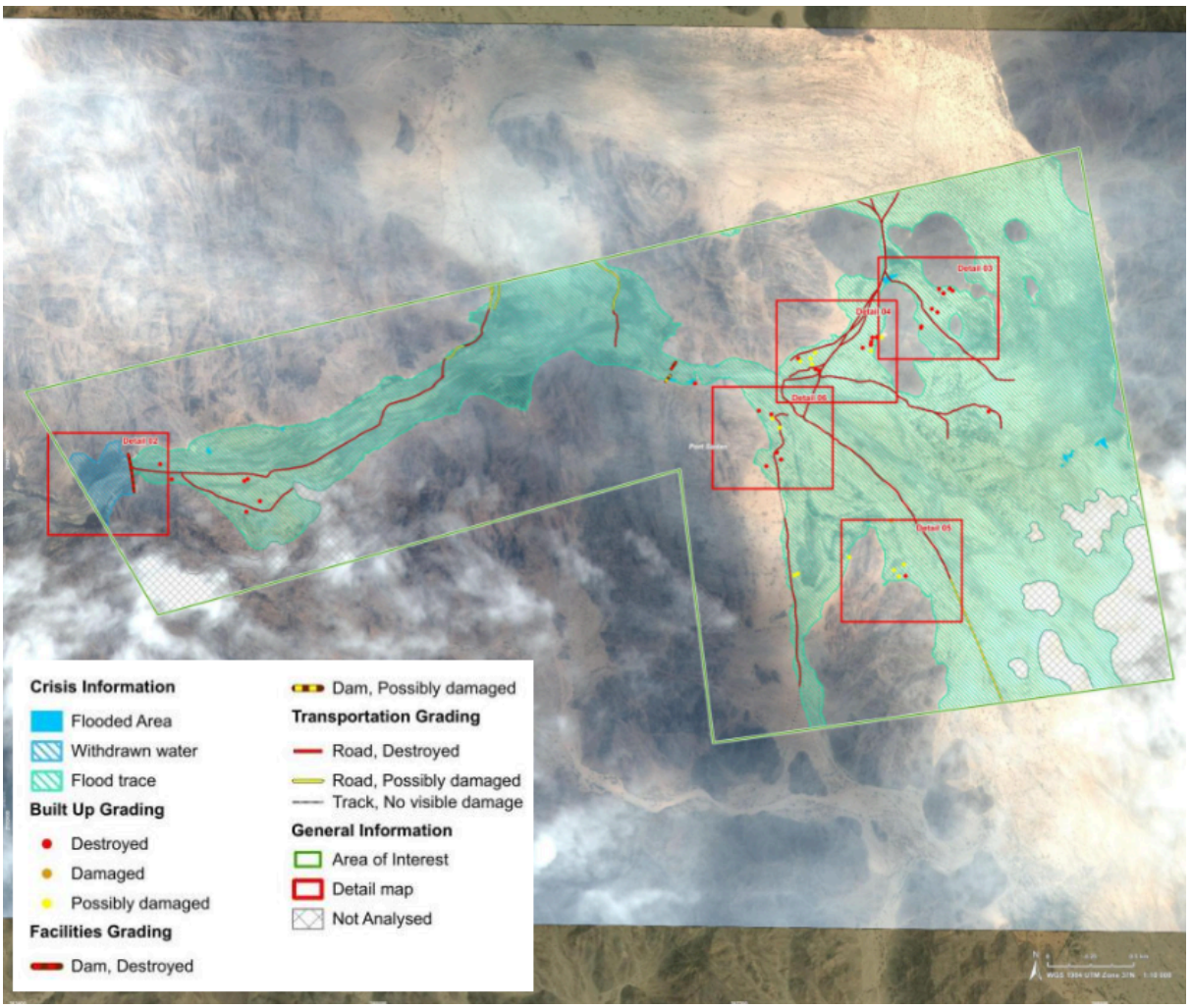

Figure 12. *Map illustrating the flooded areas of Port Sudan associated with the collapse and damage to the Arba'at Dam, as of 29 August 2024. Source: Copernicus Emergency Management Service (2024, 4 Sept).*

Adaptation efforts, including spate irrigation, have been employed in areas like the Gash River basin to utilise floodwaters for agricultural purposes (Fadul et al., 2019). However, weak institutions and limited resources have hindered broader adoption of effective flood preparedness measures. The Arba'at Dam collapse further underscores the fragility of existing water management systems, as attempts to stabilise the region were undermined by incoming waters, worsening the flood impact in downstream communities (Sudan Tribune, 2024, 28 Aug).

Similarly, the collapse of Alau Dam in northern Nigeria on 10 September, 2024, caused catastrophic flooding in Maiduguri and surrounding areas. This led to at least 30 deaths and the displacement of around 400,000 people, with up to one million residents affected (Africa News, 2024; Adeyemi et al., 2024; Olaoluwa, 2024). The worst flooding in decades, nearly half of Mauduguri was submerged, with severe damage to homes, businesses, and essential infrastructure (Olaoluwa, 2024; Africa News, 202), intensifying the existing humanitarian crisis (UNHCR, 2024).

The Lake Chad Basin borders seven countries, with a semi-arid climate and contributes water to Lake Chad. Naturally, transboundary water management issues arise, as the water is diverted for irrigation, hydropower generation and ecosystem services. Transboundary basin authorities, such as the Niger

Basin Authority, have been established in the region, in addition to the management of the different water uses, to reduce flood impact and vulnerability in their respective areas (Medinilla, 2017). However, information on transboundary floods in the region remains quite scarce.

Adaptation projects in countries like Nigeria and Chad have been criticised for being hazard-focused rather than addressing the underlying vulnerabilities that create these impacts (Epule, Chehbouni, & Dhiba, 2021). Therefore, in addressing root causes, adaptive social protection programmes are being increasingly implemented to strengthen the links between social protection, disaster risk reduction, and climate change adaptation (Daron et al., 2020). Early Warning Early Action tools such as early warning communication can also provide essential decision-making support. Additionally, improved transboundary governance is critical to accessing multilateral climate funds for transboundary investments. For example, the African Development Bank has supported countries in the Niger river to access climate funds for transboundary climate investments from the GCF and Global Environment Facility that could enhance resilient infrastructure and generate greater water benefits (IPCC, 2022). Risks crossing country boundaries underscore the need for transboundary cooperation, and formal transboundary arrangements that can mitigate risks and generate cross-border benefits (IPCC, 2022).

7.3 Spatial planning

Africa is the fastest urbanising region globally, with 40 percent of its population currently living in urban areas. This figure is projected to rise to nearly 60 percent by 2050 (Anderson, Quinchia and Curiel, 2022; Aliyu and Amadu, 2017; Urban Africa, 2022). Much of this urban growth has occurred in small towns and secondary cities, where over half of Africa's urban population resides (Cities Alliance, 2022). Despite this significant presence, secondary cities often lack resources compared to larger cities, hindering sustainable development (Roberts and Hohmann, 2014).

Land-use changes in Sudan, particularly in Khartoum, have significantly increased flood risks due to rapid urbanisation, deforestation, and reduced natural landscapes. From 2014 to 2020, built-up areas in Khartoum increased by 3.26%, while agricultural land decreased by 13.6% (El-Hamid et al., 2021). This shift has diminished natural flood barriers, reducing the landscape's capacity to absorb rainwater and increasing urban flooding risks. Recurrent flooding has also expanded water bodies by 21.4% around the White Nile and 7.28% around the Blue Nile, further exacerbating these vulnerabilities (El-Hamid et al., 2021). Mahmoud et al. (2014) emphasise that inadequate drainage infrastructure, covering only 42% of Khartoum, combined with impervious surfaces, has worsened urban flooding during extreme rainfall events. Additionally, deforestation and unsustainable agricultural practices like overgrazing have degraded soil quality in rural areas, increasing runoff and flash floods.

While sustainable measures such as rainwater harvesting (RWH) have been proposed to manage urban runoff (Mahmoud et al., 2014), their adoption remains limited due to weak institutional frameworks and inadequate investment (Horn & Elagib, 2018; Mahmoud et al., 2014). Enhancing RWH and improving drainage systems could mitigate these flood risks, but effective implementation is essential for increasing Sudan's resilience to extreme weather events.

Lack of funding contributes to challenges including inadequate urban planning and governance, substandard infrastructure, and difficulties for residents in meeting their basic needs (Rouhana &

Bruce, 2016; Aliyu & Amadu, 2017; Cities Alliance, 2022). Serious consequences include rapid development on floodplains and insufficient, sometimes non-existent drainage and waste management systems (Tazen et al., 2018; Adeleye et al., 2019; Nkwunonwo, Whitworth, & Baily, 2016; Bang, Miles, & Gordon, 2019). As urban migration increases, informal settlements are expanding, many situated in areas vulnerable to landslides, floods, sea-level rise, and storm surges, further exacerbating existing vulnerabilities (IPCC, 2022).

In the Niger River basin, settlements constructed on levees and coastal plains during the 1980s drought have led to more people living in flood-prone areas as rainfall has increased in recent decades (Ogunkoya and Olayiwola, 2022). In Nigeria, informal settlements now accommodate half of the urban population and are often located in flood-prone regions (Ali, Akoteyon, & Soladoye, 2021).

Nigeria's urban population surged from 10.1 percent in 1950 to 58.3 percent in 2020 and is projected to double over the next 20 years (Aliyu & Amadu, 2017). This trend positions Nigeria among three countries expected to account for 37 percent of global urbanisation over the next 30 years (Aliyu & Amadu, 2017). In addition to a natural population growth rate of 3.9 percent, Nigeria's urbanisation is fuelled by rural-urban migration, the development of local government area systems, the expansion of urban neighbourhoods through annexation, and the transformation of rural villages into small urban communities (Soulé et al., 2020; Aliyu & Amadu, 2017). This transformation often leads to vegetation clearing in peri-urban areas, increasing their susceptibility to flooding (Umar & Gray, 2022; Soulé et al., 2020; Elagib et al., 2021; Fiorillo et al., 2018).

7.4 Early Warning Early Action

Sudan has implemented several flood forecasting systems to manage flood risks, especially in regions prone to seasonal flooding. One such system, developed by the Ministry of Water Resources and Irrigation, focuses on the Gash River Basin and River, on which Kassala is located. The system uses satellite-based rainfall estimates, GIS, and hydrological models to provide real-time flood forecasts to farmers through Information and Communication Technology (ICT), helping them better manage their agricultural activities and prepare for flood events (Elagib et al., 2021). In the Baraka River Basin, similar efforts using GIS, land-use maps, and rainfall estimates have proven effective for flood water management and harvesting (Babker et al., 2020; Elagib et al., 2021). However, challenges remain due to data gaps and model limitations, which require bias corrections to improve the accuracy of seasonal forecasts (Lorenz et al., 2020; Elagib et al., 2021).

For 2024, the IGAD Climate Prediction and Applications Centre (ICPAC) forecasted above-average rainfall for Sudan between June and September, raising the risk of severe flooding (OCHA, 2024). This warning underscored the importance of early action to mitigate the anticipated impacts. In response, the Ministry of Health, with support from WHO and UNICEF, launched an oral cholera vaccination campaign in Kassala State in August 2024, providing 51,000 doses to protect communities in high-risk areas (OCHA, 2024). Additionally, supplies were pre-positioned, and cholera treatment units (CTUs) were established across affected regions to ensure rapid response to outbreaks (OCHA, 2024).

Guided by the National Emergency Management Agency, Nigeria began integrating disaster risk reduction into its policies and operations in 2009 (UNECA, 2015). This action has resulted in the

establishment of an early warning system for floods, with disaster preparedness and response activities now covering multiple sectors (Federal Ministry of Environment, n.d.; Mashi, Oghenejabor, and Ibrahim, 2019). While Nigeria is still developing an early action protocol (EAP) and an anticipatory humanitarian action mechanism for flooding, the Nigerian Red Cross Society received immediate Disaster Response Emergency Fund support to implement early actions (IFRC, 2022). UNDP's (2023) assessment report on the 2022 Nigeria floods suggests that not even one-fifth (19.7%) of the affected households were aware of the government's alerts about the floods, while merely 8.3% able to evacuate preemptively. It is likely that similar figures are true for the 2024 floods.

7.5 Humanitarian aid landscape

The 2024 floods in Sudan have significantly deepened the country's humanitarian crisis, straining the capabilities of aid organisations and government bodies and exacerbating vulnerabilities among affected populations. A state-level high committee, including the Sudanese Red Crescent Society (SRCS), was established to coordinate aid, monitor flood impacts, and mobilise resources (OCHA, 2024, 5 Sept). Essential responses have included providing water, sanitation, hygiene (WASH), non-food items (NFIs), and medical supplies, with the International Organization for Migration (IOM) delivering crucial support to over 214,000 individuals (IOM, 2024, 29 Aug).

However, the erosion of the protective status of humanitarian workers, including those under the Red Cross and Red Crescent emblems, has significantly hindered aid delivery, compounding the crisis. Historically respected norms that ensured the safety and neutrality of aid workers have been increasingly disregarded in the context of ongoing conflict and instability. This erosion has left aid workers vulnerable to violence and attacks, directly impacting their ability to reach communities in need (OCHA, 2024, 2 Oct). For example, safety concerns for aid convoys have delayed critical deliveries of food, water, and medical supplies to flood-affected regions, leaving populations without necessary assistance in a timely manner and increasing their susceptibility to hunger and disease. These security challenges have profound implications for flood response efforts.

Flood-related disruptions have also undermined the broader humanitarian response to Sudan's pre-existing crisis. The flooding washed away roads and bridges, blocking access to key areas like Port Sudan and Darfur and further isolating communities. In Darfur, for instance, the destruction of bridges has delayed food deliveries from the World Food Programme to famine-threatened areas like Kreinik, where displaced populations face severe shortages (Siddig et al., 2024, 27 Aug). Damage to critical infrastructure, such as communication networks, has also hampered the collection of accurate information (PressTV, 2024, 27 Aug). This breakdown in humanitarian access and coordination, combined with the erosion of protection for aid workers, has left many communities increasingly vulnerable, underscoring the urgent need for a secure and effective aid environment in Sudan.

As over 4.4 million people are estimated to be affected in the six countries, the European Union has released €5.4 million in humanitarian aid to help the most affected populations in the aftermath of the devastating floods in Chad, Nigeria and neighbouring countries (ECHO, 2024, 20 Sep). This funding will help humanitarian partners on the ground to provide immediate aid and respond to the most urgent needs concerning food, shelter, access to clean water and sanitation and other essential services in the hardest-hit areas (ECHO, 2024, 20 Sep; USAID, 2024, 18 Sep). Similarly, USAID has surged more than $3 million in humanitarian assistance thus far to help people address emergency needs,

including the $1 million provided in the immediate aftermath of the floods (USAID, 2024, 18 Sep). People in hard-hit areas in Chad are being provided with emergency cash and food assistance as WFP calls for investments in early warning systems, disaster risk financing and other measures to help mitigate flood and climate risks (UN News, 2024, 17 Sep).

In partnership with the International Committee of the Red Cross (ICRC), the Nigerian Red Cross Society (NRCS) volunteers and staff have responded through search and rescue efforts, providing first aid and medical evacuations (ICRC, 2024, 20 Sep). As part of their response, the NRCS spearheaded hygiene promotion activities in three camps hosting flood affected communities and through the cholera preparedness drive positioned contingency stock including AquaTabs and chlorine powder (ICRC, 2024, 20 Sep). The volunteers undertaking these tasks were trained to use the prepositioned materials and prioritised cleaning wells, hand pumps, boreholes and other community water sources (ICRC, 2024, 20 Sep). Other actions taken by the ICRC and NRCS included disseminating essential household items like mats, blankets, tarpaulins, kitchen kits, jerry cans, soap, hygiene kits and loincloths to affected households (ICRC, 2024, 20 Sep).

As a response to the limited roll-out of humanitarian response, communities have established self-help networks linking local neighbourhood-level responses to regional and national coordination councils (Nasir, Rhodes, & Kleinfeld, 2023; CMI, 2023). Some of these groups are called Emergency Response Rooms (ERR). ERRs provide a wide range of critical services, including, for example, medial assistance and community clinics, food distribution and community kitchens, water delivery, shelter for displaced people, restoring electricity and other basic services, and childcare and education support (The New Humanitarian, 2023). Providing essential gaps where international aid actors struggle to access, and leveraging existing social networks and community trust, ERRs build on Sudan's tradition of mutual aid and community solidarity known as "nafeer" (Shabaka, 2023). Currently, there are over 700 ERRs spread across Sudan, with more being established regularly.

V&E conclusions

Ongoing conflict and fragility is acting as a risk multiplier, on top of the existing issues of poverty, rapid urbanisation, and ageing infrastructure. In particular, conflict has created a displacement crisis in the region with millions displaced in Chad, Nigeria and Sudan, living in makeshift shelters and at higher risk when extreme rainfall triggers flooding.

The transboundary nature of the river systems in sub-saharan Africa requires coordination between neighbouring countries, which has been strained and hinders comprehensive flood management and early warning systems. Only a fraction of the population are known to have been aware of early warnings in the 2022 floods, likely to be the case in the 2024 floods. In addition, many of the same regions that were impacted by the 2022 floods had not fully recovered before they were hit again by the 2024 floods.

The low return-period of the rainfall that resulted in such severe impacts underscores the chronic, deep vulnerabilities that are driving impacts. Together, these issues create a recipe for disaster, especially as even stronger rainfall events that can be expected in the future.

To reduce flood risks, rehabilitation of damaged infrastructure should prioritise climate-smart design, including incorporating resilient materials and construction techniques and limiting construction in flood-prone areas. Effective water management, including maintaining and updating vital infrastructure like Arba'at, is crucial for mitigating both flood risks but also cascading risks on health. Finally, strengthening early warning systems by improving transboundary data sharing and ensuring greater access to warning and risk information, will be essential to reduce loss of life.

Data availability

All time series used in the attribution analysis are available via the Climate Explorer. For data that isn't, data is available upon request.

References

All references are given as hyperlinks in the text.

Appendix

A.1 Model evaluation

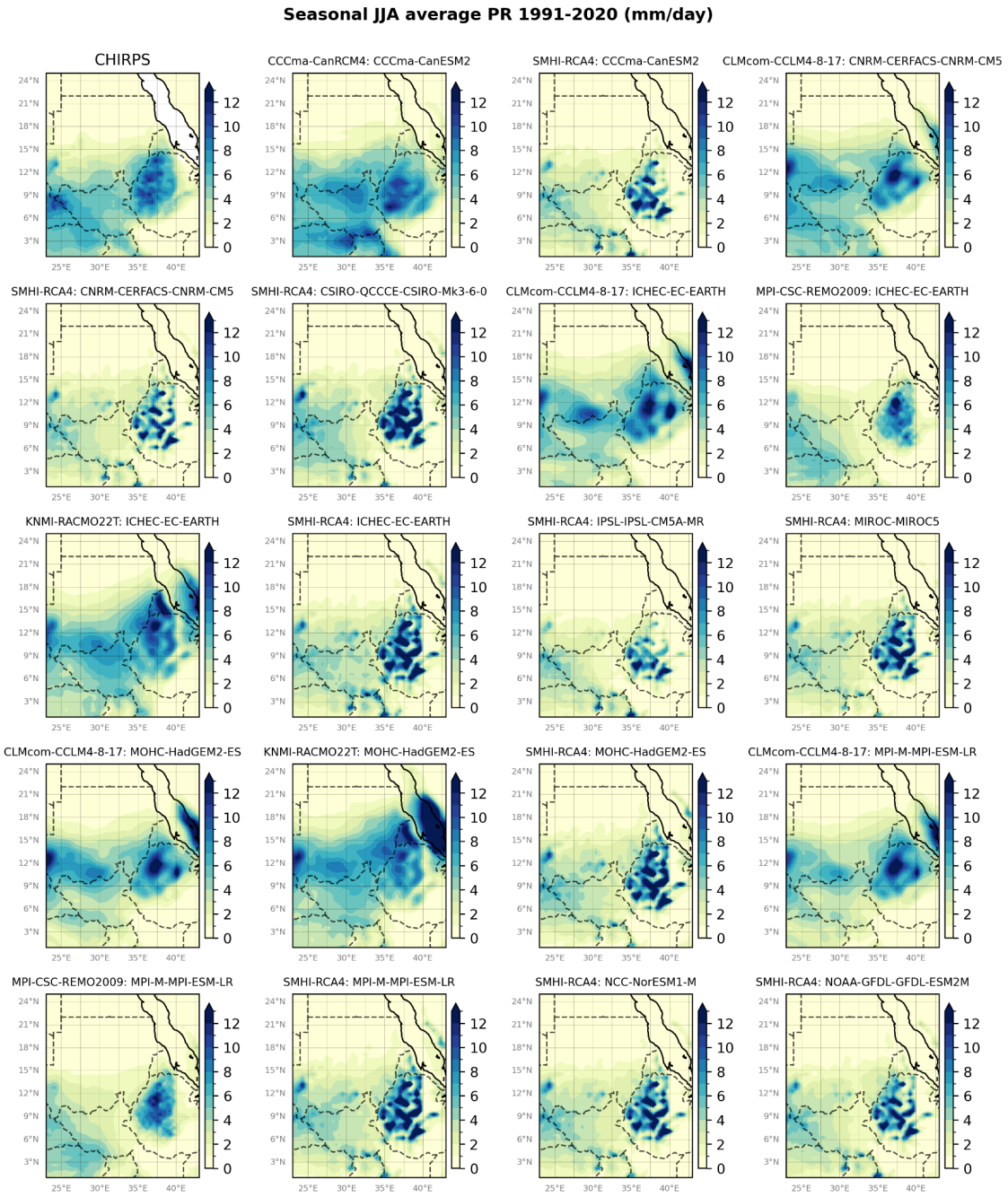

Figure A1. Evaluation of JJA average precipitation pattern from the CORDEX models.

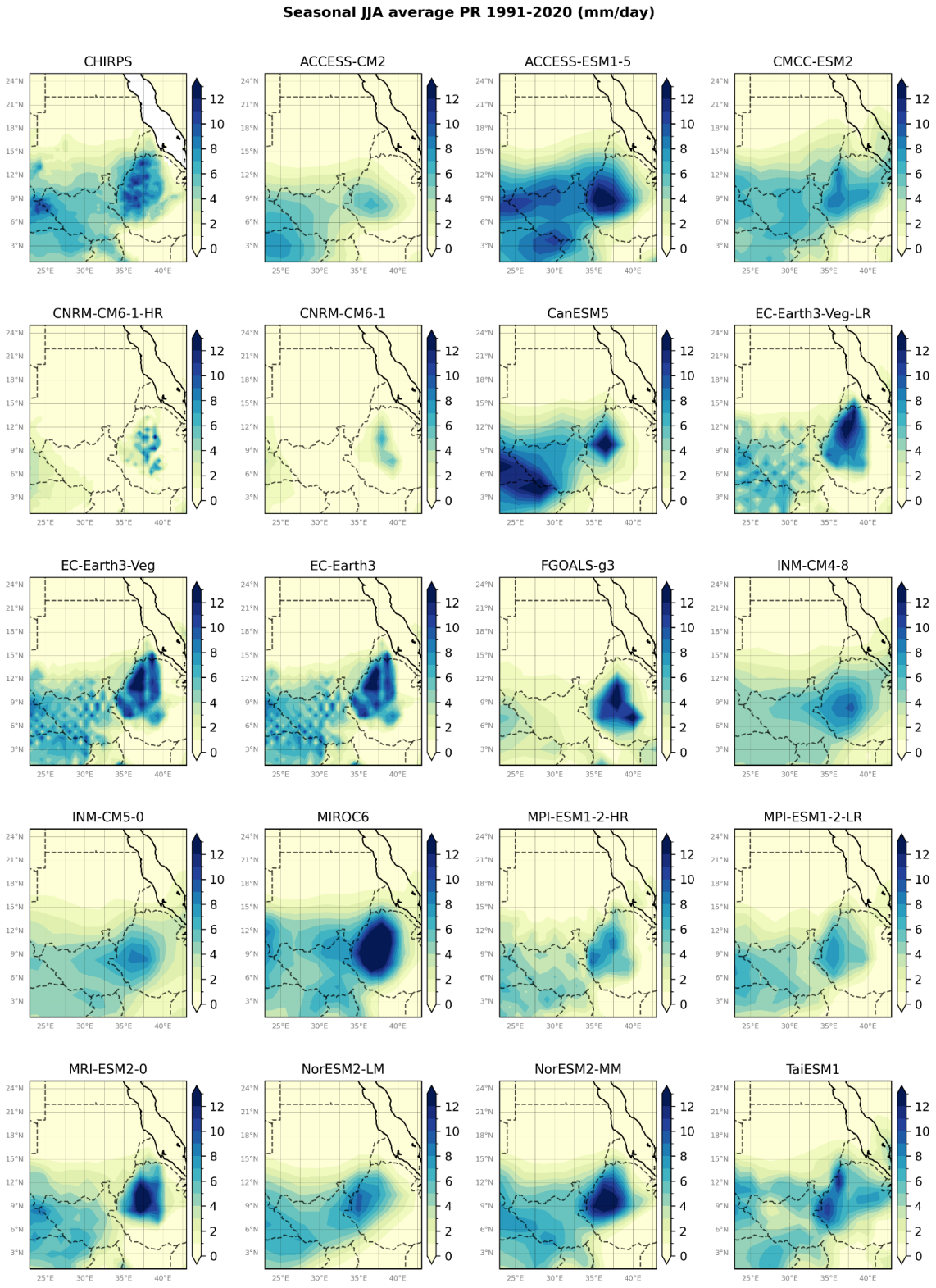

Figure A2. Evaluation of JJA average precipitation pattern from the CMIP6 models.

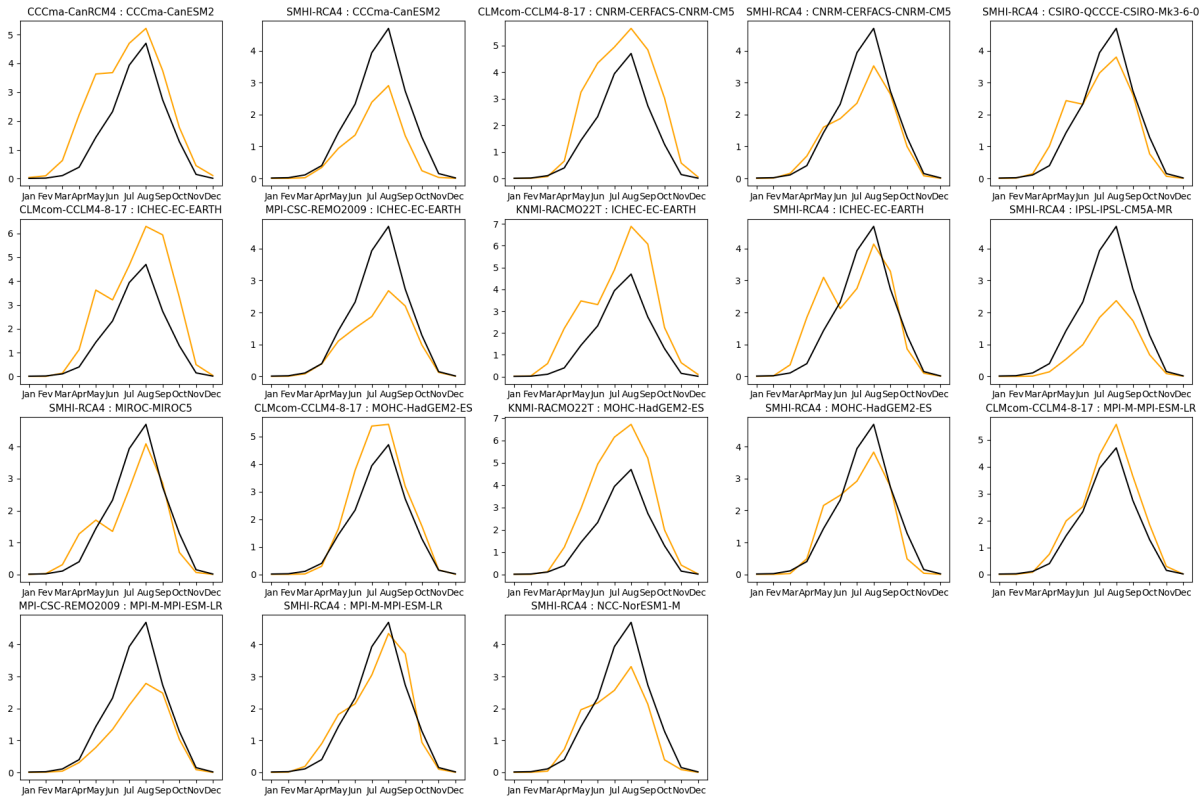

Figure A3. Evaluation of annual precipitation cycles from CORDEX models (orange lines) with CHIRPS (black line).

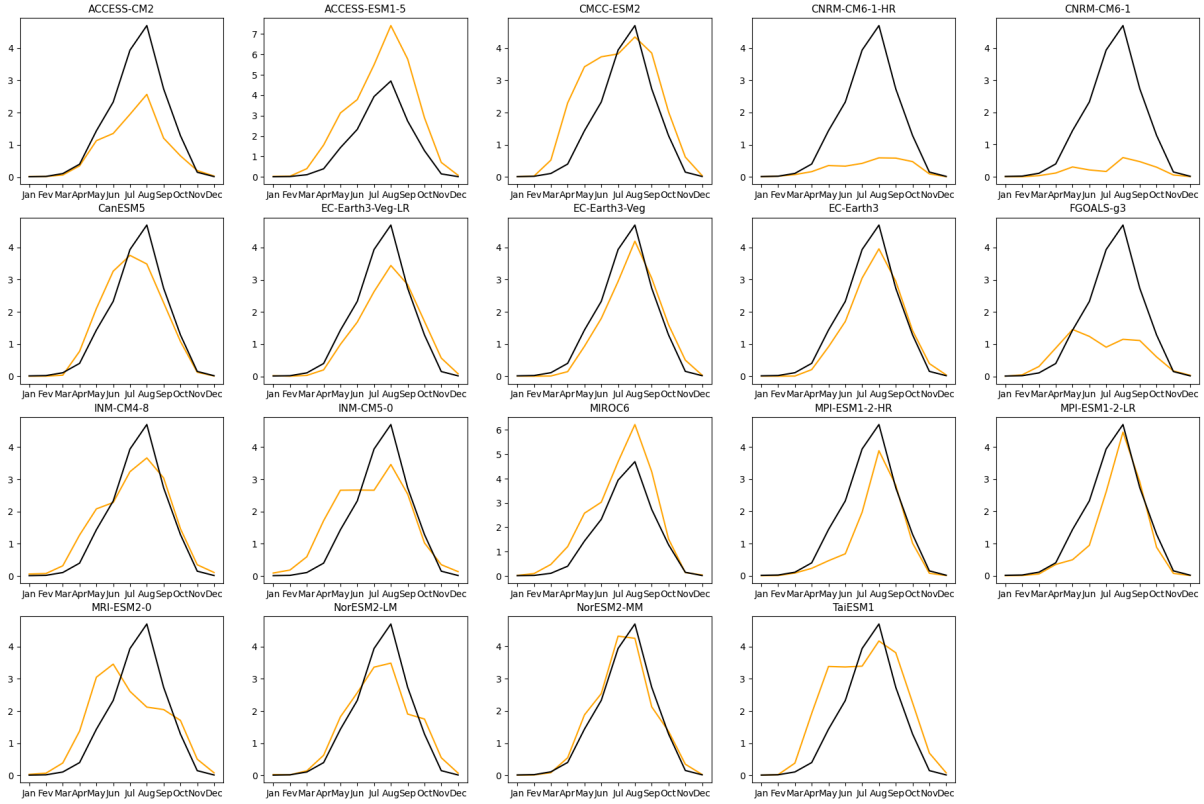

Figure A4. Evaluation of annual precipitation cycles from CMIP6 models (orange lines) with CHIRPS (black line).